

Supplemental Material

Sliding ferroelectricity and moiré effect in Janus

bilayer MoSSe

Liyan Lin,^{1,2} Xueqin Hu,^{1,2} Ruijie Meng,^{1,2} Xu Li^{3,4}, Yandong Guo,^{1,2,5,*} Yue Jiang,⁶ Dongdong Wang,^{1,2} Haixia Da,^{1,2} Yurong Yang^{3,4,*} and Xiaohong Yan^{1,2,7,*}

¹*College of Electronic and Optical Engineering, Nanjing University of Posts and Telecommunications, Nanjing 210046, China*

²*Key Laboratory of Radio Frequency and Micro-Nano Electronics of Jiangsu Province, Nanjing 210023, China*

³*National Laboratory of Solid State Microstructures and Collaborative Innovation Center of Advanced Microstructures, Department of*⁴*Materials Science and Engineering, Nanjing University, Nanjing 210093, China*

⁵*College of Natural Science, Nanjing University of Posts and Telecommunications, Nanjing 210046, China*

⁶*College of Science, Jinling Institute of Technology, Nanjing 211169, China*

⁷*Jiangsu University, Zhenjiang 212013, China*

Table S1. The relaxed lattice parameters, and structural parameters such as bond lengths and bond angles of the Janus bilayer MoSSe structure with AA stacking. The parameter D represents the interlayer distance between the nearest neighboring atomic layers of the upper and lower layers.

| configuration | Lattice parameter | | Bond length (Å) | | Angle (°) | | D (Å) | |
|---------------|-------------------|--|-----------------|-------|----------------------|---------------------|-------|-----------------------|
| | a=b | | Mo-S | Mo-Se | $\angle\text{SMoSe}$ | $\angle\text{SMoS}$ | | $\angle\text{SeMoSe}$ |
| Se-Se | 3.22 | | 2.41 | 2.52 | 82.08 | 83.83 | 79.25 | 3.73 |
| S-S | 3.22 | | 2.41 | 2.52 | 82.01 | 83.94 | 79.25 | 3.55 |
| S-Se | 3.22 | | 2.41 | 2.52 | 82.04 | 83.92 | 79.22 | 3.64 |

Table S2. The energy difference of AB stacking for S-S, Se-Se, and S-Se configurations. The parameter D represents the interlayer distance between the nearest neighboring atomic layers of the upper and lower layers.

| Structure | AB stacking | | |
|------------------|-------------|-------|------|
| | Se-Se | S-S | S-Se |
| ΔE (meV) | 0 | 13.78 | 0.30 |
| D (Å) | 3.24 | 2.99 | 3.08 |

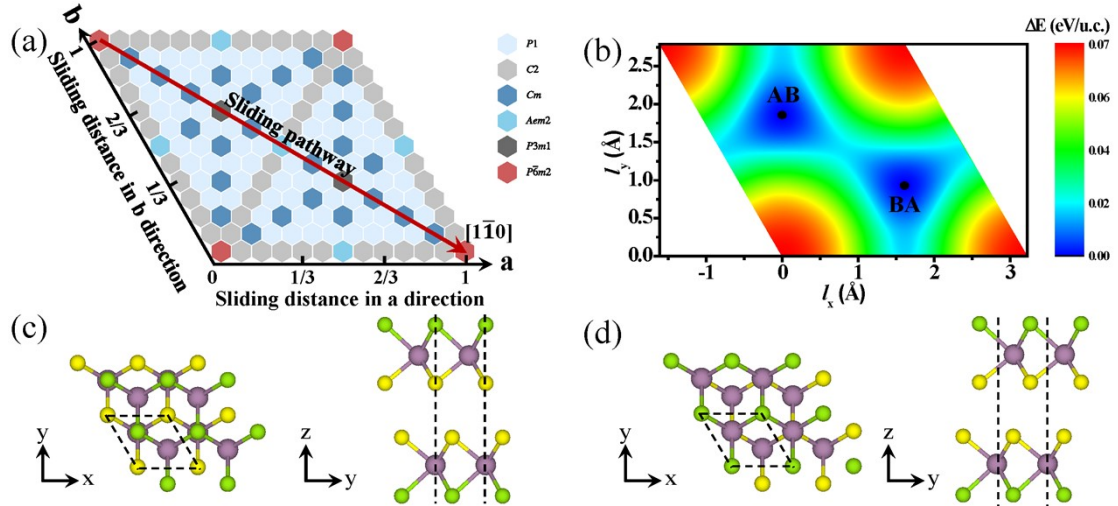


Fig. S1. (a) Illustration of the structural space group of the S-S configuration sliding in the ab -plane. Each honeycomb data point represents a slided structure. Different colors indicate different space groups. (b) The energy contour plot of bilayer Se-Se configuration versus the sliding distance (l_x , l_y). The contour colors illustrate the energy difference of the unit cell relative to the energy of ground state (AB stacking and BA stacking). (c)-(d) The top and side views of the two lowest-energy ground-state structures in Fig. S1(b), the AB stacking and the BA stacking, respectively.

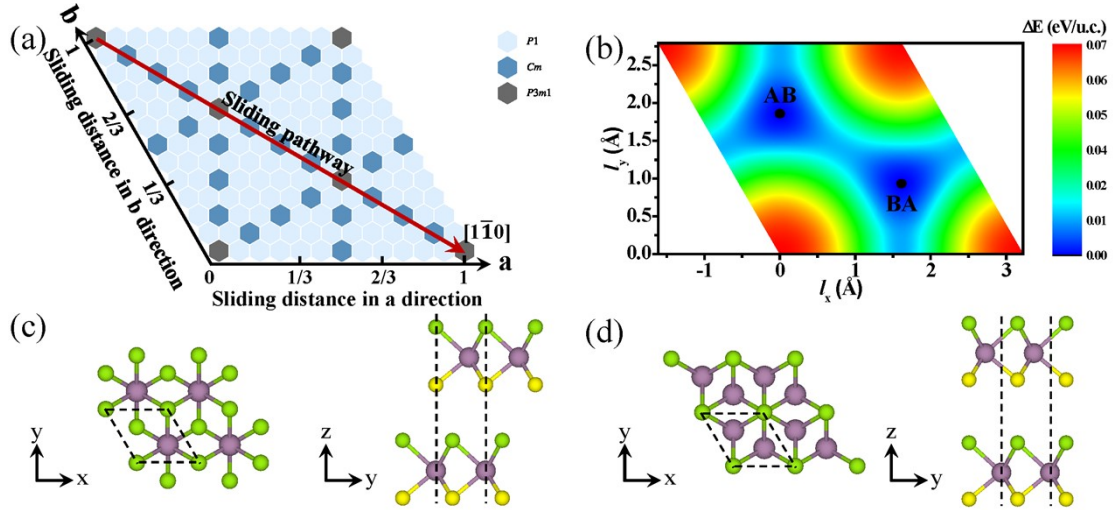


Fig. S2. (a) Illustration of the structural space group of the S-Se configuration sliding in the ab -plane. Each honeycomb data point represents a slided structure. Different colors indicate different space groups. (b) The energy contour plot of bilayer Se-Se configuration versus the sliding distance (l_x , l_y). The contour colors illustrate the energy difference of the unit cell relative to the energy of ground state (AB stacking and BA stacking). (c)-(d) The top and side views of the two lowest-energy ground-state structures in Fig. S2(b), the AB stacking and the BA stacking, respectively.

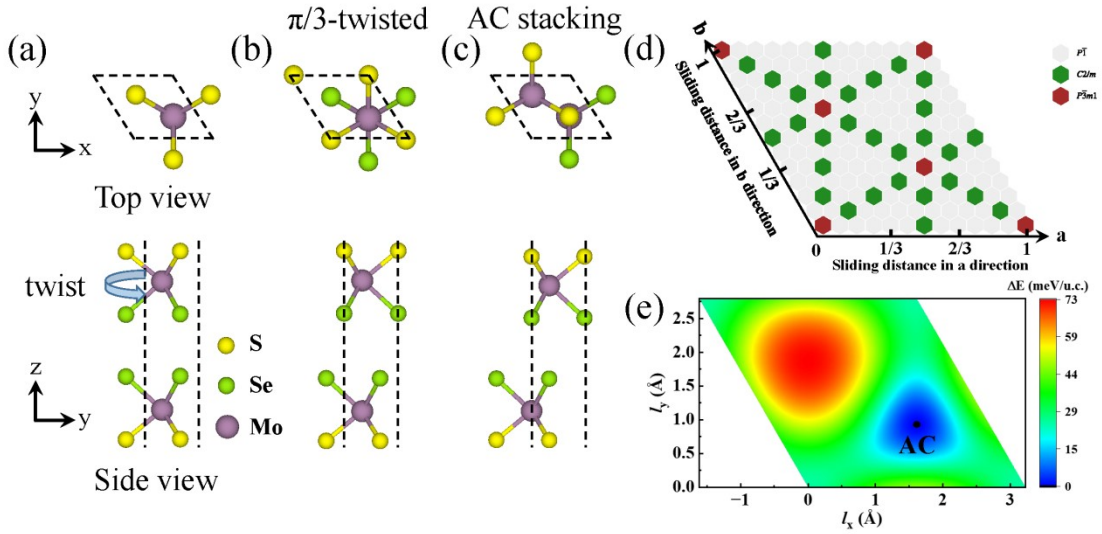


Fig. S3. (a)-(b) The top and side views of untwisted and $\pi/3$ -twisted of AA stacking structures in Se-Se configuration. (c) The top and side views of AC stacking. (d) Illustration of the structural space group of the $\pi/3$ -twisted Se-Se configuration sliding in the ab plane. Each honeycomb data point represents a slided structure. Different colors indicate different space groups. (e) The energy contour plot of bilayer Se-Se configuration versus the sliding distance (l_x , l_y). The contour colors illustrate the energy difference of the unit cell relative to the energy of ground state (AC stacking).

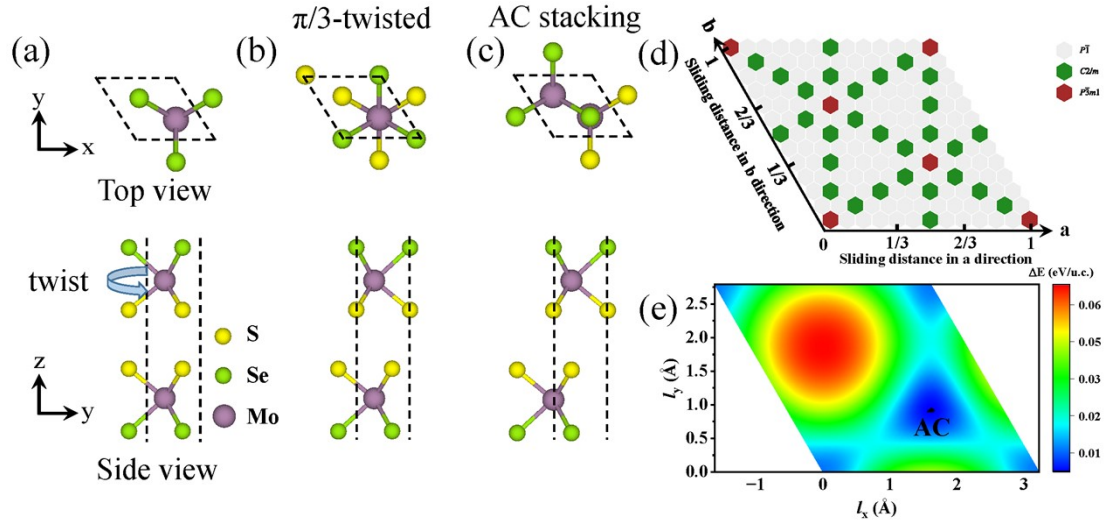


Fig. S4. (a)-(b) The top and side views of untwisted and $\pi/3$ -twisted of AA stacking structures in S-S configuration. (c) The top and side views of AC stacking. (D) Illustration of the structural space group of the $\pi/3$ -twisted S-S configuration sliding in the ab plane. Each honeycomb data point represents a slided structure. Different colors indicate different space groups. (E) The energy contour plot of bilayer S-S configuration versus the sliding distance (l_x , l_y). The contour colors illustrate the energy difference of the unit cell relative to the energy of ground state (AC stacking).

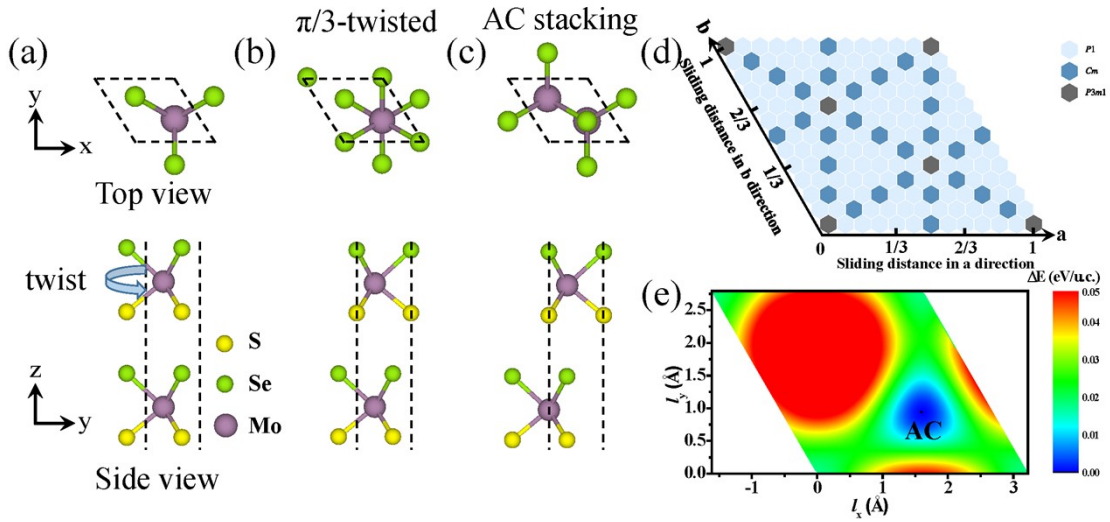


Fig. S5. (a)-(b) are the top and side views of untwisted and $\pi/3$ -twisted of AA stacking structures in S-Se configuration. (c) The top and side views of AC stacking. (d) Illustration of the structural space group of the $\pi/3$ -twisted S-Se configuration sliding in the ab plane. Each honeycomb data point represents a slided structure. Different colors indicate different space groups. (e) The energy contour plot of bilayer S-Se configuration versus the sliding distance (l_x , l_y). The contour colors illustrate the energy difference of the unit cell relative to the energy of ground state (AC stacking).

Table S3. The interlayer distance (D) and out-of-plane polarization (OP) of the optimized AB stacking are corrected with different vdW functionals.

| Configuration | OP & D (pC/m) & (Å) | vdW functional | | | | | |
|---------------|---------------------------|----------------|--------|---------|-------------|------------|------------|
| | | DFT-D3 | DFT-D2 | vdW-DF2 | optB86b-vdW | optB88-vdW | optPBE-vdW |
| Se-Se | OP | -0.42 | -0.45 | -0.25 | -0.45 | -0.40 | -0.28 |
| | D | 3.24 | 3.23 | 3.49 | 3.22 | 3.27 | 3.422 |
| S-S | OP | -0.84 | -0.77 | -0.55 | -0.87 | -0.79 | -0.58 |
| | D | 3.00 | 3.04 | 3.20 | 2.98 | 3.02 | 3.16 |

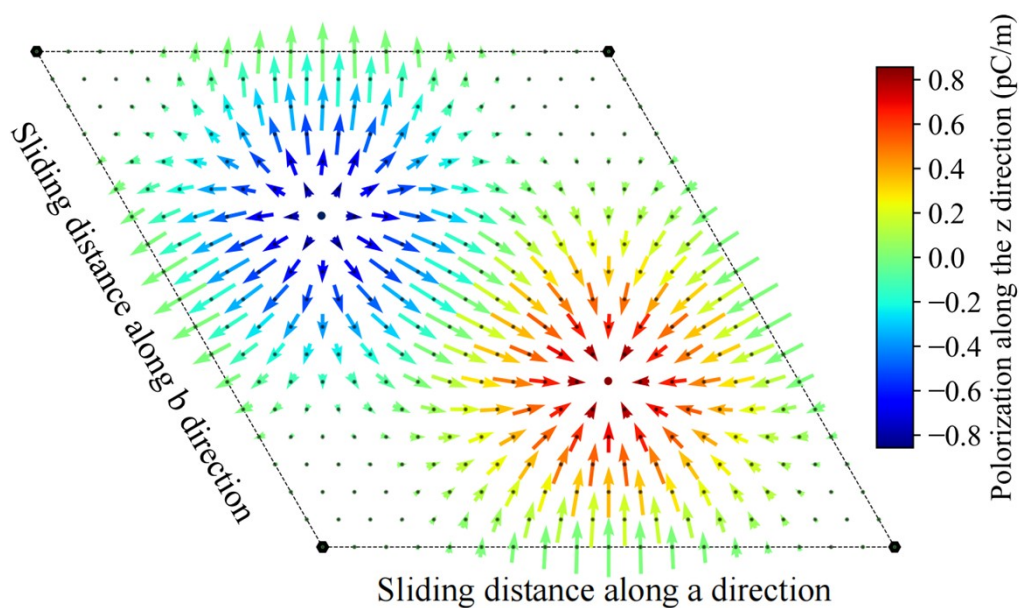


Fig. S6. Diagram of in-plane and out-of-plane polarization of sliding structures for S-S configuration. The color contour map shows the magnitude and direction of out-of-plane polarization. The arrow indicates the direction of in-plane polarization. The length of the arrows in the diagram represents the magnitude of the in-plane polarization, with longer arrows indicating a greater polarization. The longest arrow signifies the maximum in-plane polarization of 1.28 pC/m.

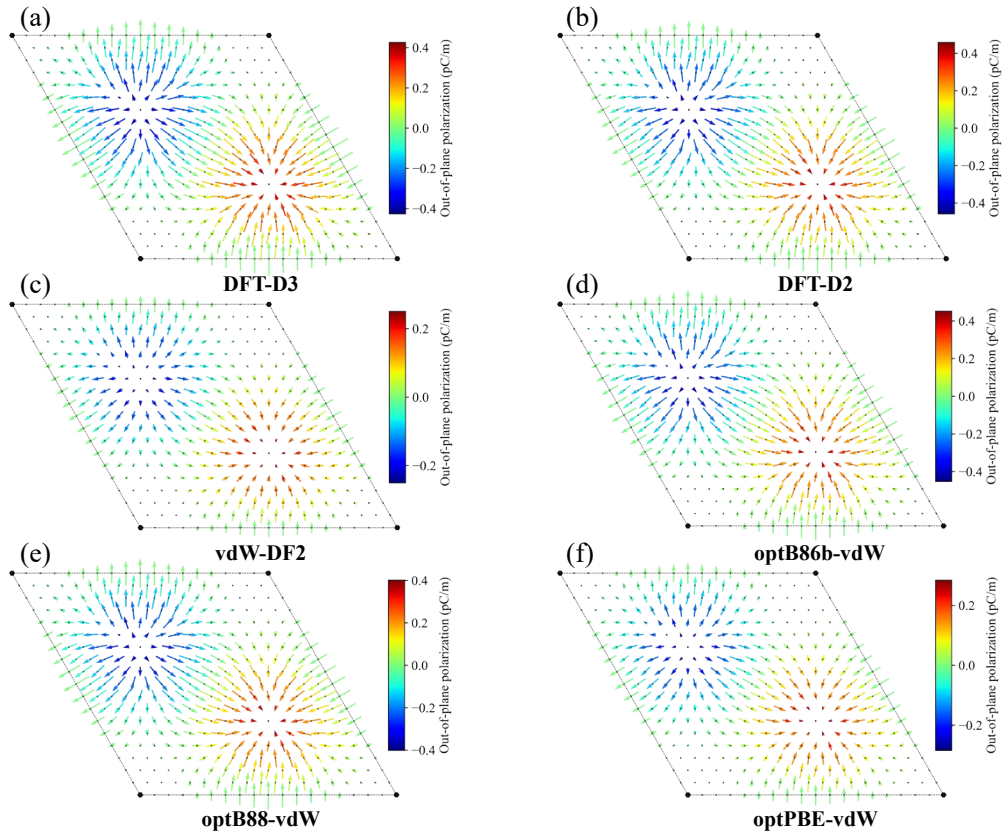


Fig. S7. The in-plane and out-of-plane polarization of the sliding structure in the Se-Se configuration, were computed using six different vdW functionals, specifically (a) DFT-D3, (b) DFT-D2, (c) vdW-DF2, (d) optB86b-vdW, (e) optB88-vdW, and (f) optPBE-vdW, respectively. The color contour map shows the magnitude and direction of out-of-plane polarization. The arrow indicates the direction of in-plane polarization. The length of the arrows in the diagram represents the magnitude of the in-plane polarization, with longer arrows indicating a greater polarization.

Table S4. Predicted 2D sliding ferroelectric. The " P_{\perp} " symbol denotes out-of-plane polarization. And the " P_{\parallel} " denotes in-plane polarization.

| Materials | P_{\perp} | P_{\parallel} | Thickness |
|--------------------------------------|-------------|-----------------|-----------|
| BN [1] | 2.08 pC/m | - | Bilayer |
| InSe [1] | 0.24 pC/m | - | Bilayer |
| MoS ₂ [1] | 0.97 pC/m | - | Bilayer |
| GaSe [1] | 0.46 pC/m | - | Bilayer |
| GaN [1] | 9.72 pC/m | - | Bilayer |
| MoSi ₂ N ₄ [2] | 3.36 pC /m | - | Bilayer |
| MoGe ₂ N ₄ [2] | 3.05 pC/m | - | Bilayer |
| CrSi ₂ N ₄ [2] | 2.49 pC/m | - | Bilayer |
| WSi ₂ N ₄ [2] | 3.44 pC/m | - | Bilayer |
| BP [3] | 1.07 pC/m | - | Bilayer |
| BAs [3] | 0.96 pC/m | - | Bilayer |
| BSb [3] | 3.70 pC/m | - | Bilayer |
| AlN [3] | 7.19 pC/m | - | Bilayer |
| GaN [3] | 5.76 pC/m | - | Bilayer |
| InN [3] | 13.83 pC/m | - | Bilayer |
| SiC [3] | 2.89 pC/m | - | Bilayer |
| GeC [3] | 2.78 pC/m | - | Bilayer |
| SnC [3] | 4.41 pC/m | - | Bilayer |
| MnSe [4] | 2.70 pC/m | - | Bilayer |
| MoSe ₂ [5] | 0.59 pC/m | - | Bilayer |
| WS ₂ [5] | 0.69 pC/m | - | Bilayer |
| WSe ₂ [5] | 0.73 pC/m | - | Bilayer |
| MoSSe-SS (AB stacking) | 0.86 pC/m | - | Bilayer |
| MoSSe-SS (TS stacking) | - | 1.2 pC/m | Bilayer |

[1] Li, Lei and Menghao Wu. Binary compound bilayer and multilayer with vertical polarizations: Two-dimensional ferroelectrics, multiferroics, and nanogenerators. ACS nano 11 6 (2017): 6382.

[2] Zhong, Tingting et al. Sliding ferroelectricity in two-dimensional MoA₂N₄ (A = Si or Ge) bilayers: high polarizations and Moiré potentials. Journal of Materials Chemistry A 9 35 (2021): 19659.

[3] Wang, Zhe et al. Sliding ferroelectricity in bilayer honeycomb structures: A first-principles study. Physical Review B 107 3 (2023): 035426.

[4] Liu, Kehan et al. Tunable sliding ferroelectricity and magnetoelectric coupling in two-dimensional multiferroic MnSe materials. npj Computational Materials 9 (2023): 1.

[5] Jafari, Hodayoun et al. Robust Zeeman-type band splitting in sliding ferroelectrics. arXiv 2308 (2023): 15241.

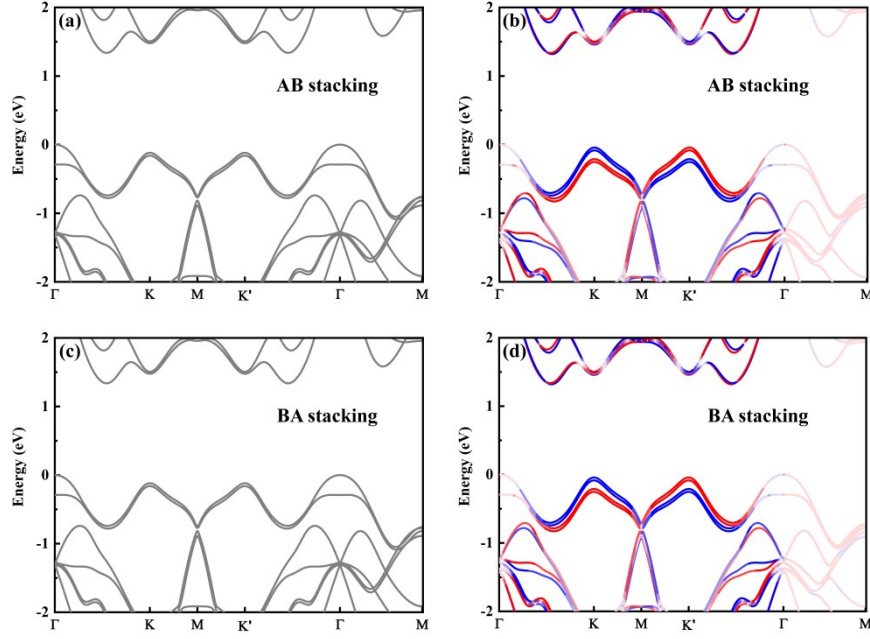


Figure R8. The electronic band structures of Se-Se configuration. (a) and (b) are the electronic band structures for AB stacking with PBE and PBE+SOC, respectively. (c) and (d) are the electronic band structures for BA stacking with PBE and PBE+SOC, respectively. The color depth indicates the quantity of the projected contribution.

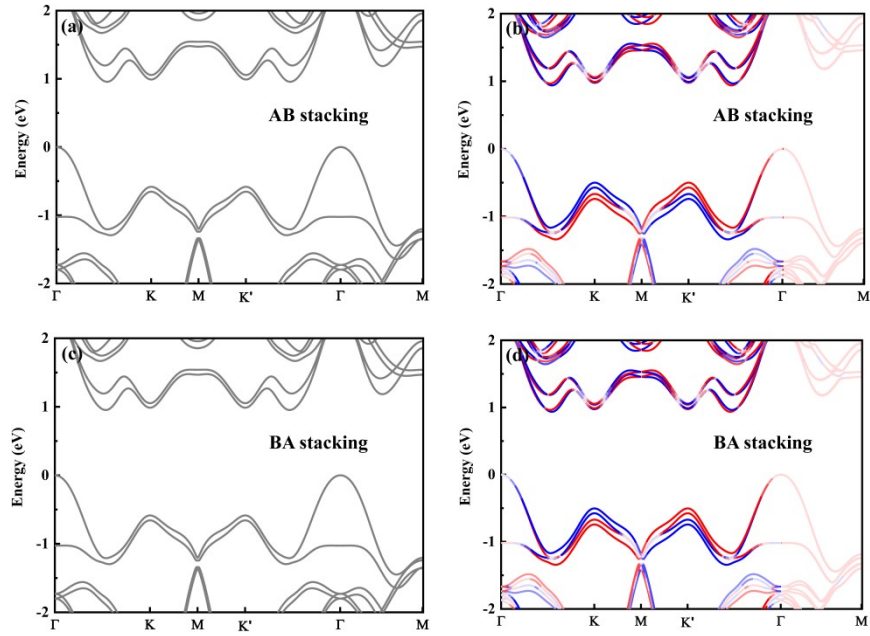


Figure S9. The electronic band structures of S-S configuration. (a) and (b) are the electronic band structures for AB stacking with PBE and PBE+SOC, respectively. (c) and (d) are the electronic band structures for BA stacking with PBE and PBE+SOC, respectively. The color depth indicates the quantity of the projected contribution.